Immunity, Vol. 13, 475–484, October, 2000, Copyright ©2000 by Cell Press

Conversion of a T Cell Antagonist into an Agonist by Repairing a Defect in the TCR/Peptide/MHC Interface: Implications for TCR Signaling

Brian M. Baker,* Susan J. Gagnon,‡ William E. Biddison,‡ and Don C. Wiley*†§
*Department of Molecular and Cellular Biology
Harvard University
Cambridge, Massachusetts 02138
†Howard Hughes Medical Institute
7 Divinity Avenue
Cambridge, Massachusetts 02138
‡Molecular Immunology Section
Neuroimmunology Branch
National Institute of Neurological Disorders and Stroke
National Institutes of Health
Bethesda, Maryland 20892

Summary

The structure of the A6 αβTCR/HTLV-1 Tax-peptide/MHC I complex with proline 6 of Tax substituted with alanine (P6A), an antagonist, is nearly identical to the structure with wild-type Tax agonist. Neither the proline in the agonist nor the alanine in the antagonist is contacted by the αβTCR. Here, we demonstrate that antagonist activity of P6A is associated with low affinity of the A6 αβTCR for Tax-P6A/HLA-A2. We show that stepwise repair of a packing defect in the TCR/MHC interface using N-alkylated amino acids results in stepwise increases in TCR affinity and activity. Kinetic and thermodynamic measurements suggest that for some ligands the range of T cell outcomes does not correlate with either their αβTCR affinity or the half-life of the αβTCR/peptide/MHC complex.

Introduction

Binding of the TCR to class I or class II MHC molecules complexed with peptide is necessary for T cell activation and initiation of a cell-mediated immune response. Simple alterations to antigenic peptides can result in a range of effects from loss of TCR signaling to weak or partial signaling or to the phenomenon of TCR antagonism (Sloan-Lancaster and Allen, 1996). Antagonist peptides do not normally produce any of the outcomes associated with activation but result in an inhibition of the T cell response when the cell is subsequently challenged with an activating agonist peptide.

Binding measurements for a variety of αβTCR/peptide/MHC interactions suggest that the range of T cell responses results from differences in either TCR affinity or dissociation rate (e.g., Matsui et al., 1994; Alam et al., 1996; Lyons et al., 1996; Kersh et al., 1998). According to these suggestions, low affinity or rapidly dissociating interactions would behave as antagonists, higher affinity or longer-lived interactions as strong agonists, and weak and partial agonists would fall between these extremes.

§To whom correspondence should be addressed (e-mail: dcwadmin@crystal.harvard.edu).

This view is supported by the data of Lyons et al. (1996), in which the binding of the mouse αβTCR 2B4 to the mouse class II MHC I-E^k complexed with six altered peptides (one agonist, two weak agonists, and three antagonists) was investigated. The conclusion was that the TCR recognized the agonist ligand with the strongest affinity and slowest off rate (longest half-life), followed by the weak agonists, which were recognized with intermediate affinities and off rates. The antagonist ligands in turn were recognized with the weakest affinity and the fastest off rates, although it was necessary to measure dissociation rates for the antagonists with an indirect method (van der Merwe et al., 1994). Kersh et al. (1998) presented a stronger correlation between TCR activity and dissociation rate, reporting kinetics and affinities for the mouse αβTCR 3.L2 binding to the class II MHC I-E^k complexed with four altered peptides (a full agonist, a weak agonist, a weak agonist/antagonist, and an antagonist). Although the ligands were reported to have similar TCR affinities, there was more variability among the dissociation rates, with the antagonist ligand dissociating the fastest and the agonist the slowest. As discussed by the authors, however, only very small portions of the kinetic data could be fit to determine rates. Also, the Biacore data, as presented, were not corrected for bulk refractive index changes, contributing to disagreement between affinities determined from kinetic and equilibrium experiments (Myszka, 1999). A correlation between TCR activity and dissociation rate was questioned by Alam et al. (1996), who characterized the binding of the mouse αβTCR 42.12 to the class I MHC H-2K^b complexed with four altered peptides (one agonist, one weak agonist, and two antagonists). As with the data of Lyons et al. (1996), a correlation was found between activity and affinity, with the antagonist ligands having the weakest TCR affinity, the weak agonist ligands intermediate, and the agonist ligands the strongest. However, a poorer correlation was observed between activity and dissociation rate, as the TCR/peptide/MHC complex with one of the antagonist peptides had a half-life almost twice as long as that observed with the weak agonist. This prompted the authors to suggest that correlations observed between activity and dissociation rate may be coincidental, reflecting an underlying correlation with affinity.

X-ray crystallographic structures of αβTCR/peptide/MHC complexes suggest that the entire range of TCR-initiated signals, including antagonism, weak agonism, and full agonism, can be generated with only minor differences in either the conformation of the bound TCR or its diagonal binding mode to peptide/MHC. Three crystallographic structures of the human A6 αβTCR complexed with the class I MHC molecule HLA-A2, presenting singly substituted peptides derived from the HTLV-1 Tax peptide (LLFGYPVYV) with partial agonist and antagonist activities, are nearly identical to each other and the αβTCR/Tax/HLA-A2 complex (Garboczi et al., 1996a; Ding et al., 1999). The minor structural differences observed do not correlate with the T cell response generated; in fact, the two most closely related

structures are an antagonist and a strong agonist (Ding et al., 1999). Comparison of two different peptides, one an agonist (SIYR) and the other a weak agonist self-peptide (dEV8), in the murine 2C-αβTCR/peptide/H-2K^b complex, also showed only local conformational adjustments, like those between the Tax agonist and the weak agonist Tax-V7R, where CDR loops rearranged to accommodate the differences in the peptide sequence (Ding et al., 1999; Degano et al., 2000). Both human and mouse αβTCR structural studies involved potent agonists: Tax (an HTLV-1 peptide) stimulates 50%-maximum lysis of HLA-A2 target cells by the 2G4 T cell in the range of 1 to 10 pM peptide concentration (Ding et al., 1998, 1999), and SIYR (derived from a peptide library) stimulates 50%-maximum lysis of H-2Kb targets or 50%-maximum IL-2 production in the range of 10 to 100 pM (Udaka, 1996; Degano, 2000). The weak agonists in those studies are ~1000- to 100,000-fold less potent, and the antagonists in the human study showed no agonist activity at 1,000,000-fold higher concentrations than the ½-maximal dose of the Tax agonists. Thus, the full spectrum of activities were included in the human study and a subset, in the agonist range, in the murine study (Ding et al., 1999; Degano et al., 2000).

Of the three human αβTCR/altered-peptide/HLA-A2 structures, the one most similar to the structure with the wild-type Tax peptide agonist complex (Garboczi et al., 1996a) is an antagonist complex with the peptide substitution proline 6 to alanine (P6A). The only significant difference between the αβTCR/peptide/HLA-A2 structures with the wild-type and P6A-substituted Tax peptides is a packing defect consisting of an enlarged cavity partially filled with a bound water molecule (Ding et al., 1999). Here, we investigate how this packing defect in the interface between the A6 αβTCR and the P6A/HLA-A2 complex affects TCR binding and signaling. We find that the affinity of the A6 αβTCR for P6A/HLA-A2 is very low (116 μM), possibly resulting from a fast dissociation rate. Using structure-based design, we show that as we attempt to "repair" the packing defect with N-alkyl amino acid substitutions at peptide position 6, αβTCR affinity increases, and with rising affinity, antagonism disappears and is replaced by weak and then full agonism. However, measurements of the binding of the A6 αβTCR to HLA-A2 complexed with those N-alkylated P6 peptides with strong agonist behavior suggest that the range of T cell outcomes does not correlate directly with either the affinity or half-life. The possibility that ligands whose potency does not correlate with measurements on isolated αβTCR would show different kinetic and thermodynamic effects on membrane-bound oligomeric TCR complexes that might explain their potency in cellular assays is discussed.

Results

The Low Affinity of the A6 αβTCR for the Antagonist Ligand P6A/HLA-A2 Was Measured by Sedimentation Equilibrium Analytical Ultracentrifugation

In the X-ray structure of the complex between the A6 αβTCR, Tax peptide, and HLA-A2, the T cell receptor does not contact the proline at position 6 of the peptide (closest approach is 4.1 Å) (Garboczi et al., 1996a). The

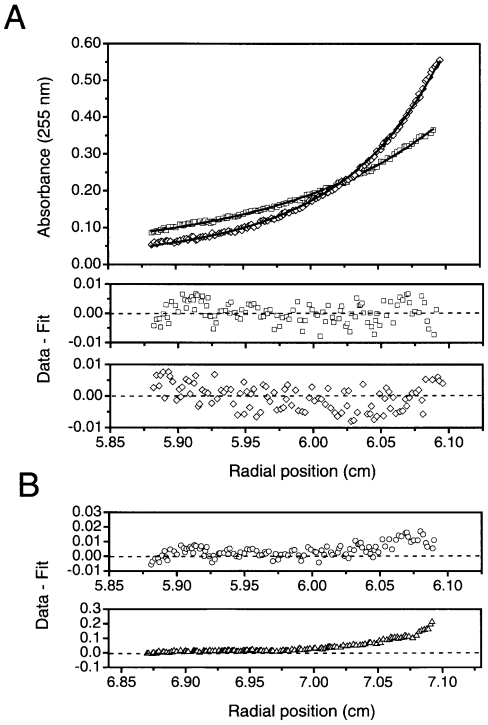

Figure 1. Representative Centrifugation Data

(A) Data for 3.2 μM TCR + 3.3 μM P6A/HLA-A2 (squares, K_D = 116 μM) and 2.9 μM TCR + 3.2 μM Tax wild-type/HLA-A2 (diamonds, K_D = 1.1 μM) centrifuged at 15,000 rpm. Lines represent fits to a 1:1 binding model. Residuals (difference between data and fitted curve) are beneath the data.

(B) Residuals for TCR binding to P6A/HLA-A2 assuming no interaction (circles, 3.2 μM TCR + 3.3 μM P6A/HLA-A2, representing 1.4% complex; triangles, 9.3 μM TCR + 9.5 μM P6A/HLA-A2, representing 3.6% complex). The large-scale and upward deflection of the points indicates the inadequacy of the fit (compare to residuals in [A], fit to a binding model).

substitution of proline 6 with alanine (P6A) changes the peptide into an antagonist (Ding et al., 1999). Remarkably, the structure of the A6 αβTCR/P6A/HLA-A2 complex is virtually identical to the structure of the complex with wild-type Tax peptide (rmsd of 0.47 Å for interacting TCR/MHC domains and 0.94 Å for peptides) (Ding et al., 1999). Since P6A/HLA-A2 remains an agonist ligand for a second HLA-A2/Tax specific αβTCR, B7, it is unlikely that the P6A substitution affects peptide binding or conformation (Hausmann et al., 1999).

In our previous study, the affinity of the αβTCR A6 for HLA-A2/Tax at 25°C was determined as ~1 μM with surface plasmon resonance (Biacore) experiments (Ding et al., 1999). However, we were unable to detect TCR binding to HLA-A2 complexed with the P6A peptide, indicating a weak affinity. Sedimentation equilibrium analytical ultracentrifugation, well suited for characterizing weak equilibria, was thus used to characterize this interaction. Figure 1A shows centrifugation of a mixture of the A6 αβTCR and P6A/HLA-A2 along with a fit to a 1:1 binding model; the residuals below the plot indicate a good fit to the model with a K_D of 116 μM (Table 1). Analyzing the data with the TCR/peptide/MHC affinity constrained as a negligible value (i.e., assuming no inter-

Table 1. Thermodynamic and Kinetic Parameters at 25°C for the A6 αβTCR Binding to HLA-A2 with Position 6 Tax Variants

Tax Peptide	K_D Ultracentrifuge (μM)	K_D Biacore Equilibrium (μM)	k_{on} (M^{-1} s^{-1})	k_{off} (s^{-1})	$t_{1/2}$ (s)[a]	k_{off}/k_{on} (μM)
Wild-type[b]	1.1 ± 0.1	0.82 ± 0.08	1.1 ± 0.1 × 10^5	0.093 ± 0.002	7.5 ± 0.2	0.9 ± 0.1
P6A[c]	116 ± 34					
P6MeG[d]	26 ± 9	27 ± 11				
P6EtG	2.1 ± 0.3	4.2 ± 0.6	0.66 ± 0.02 × 10^5	0.23 ± 0.01	3.0 ± 0.2	3.5 ± 0.3
P6PrA[e]		2.5 ± 0.1	0.31 ± 0.05 × 10^5	0.067 ± 0.005	10.3 ± 0.8	2.2 ± 0.4

[a] $t_{1/2} = 0.693/k_{off}$.
[b] Biacore data for wild-type Tax from Ding et al., 1999.
[c] No TCR binding with P6A was observed in Biacore experiments (Ding et al., 1999).
[d] The TCR dissociation rate with P6MeG was too fast to obtain accurate kinetics.
[e] Analytical ultracentrifugation was not performed with P6PrA.

action) results in significant deviations in the residuals (Figure 1B), demonstrating the utility of analytical ultracentrifugation in resolving this weak affinity. Figure 1A also shows a centrifuge binding experiment using wild-type Tax peptide; the K_D of 1.1 μM obtained is in excellent agreement with the values from our previous Biacore experiments (~1 μM; Table 1).

Our inability to detect TCR binding with the P6A peptide using Biacore is likely due to a rapid TCR dissociation rate. Interactions between TCR and MHC/peptide molecules with affinities close to or weaker than 100 μM have been characterized with Biacore (Lyons et al., 1996; B. B. and D. W., unpublished data), but, in those cases, the interactions have slow dissociation rates, allowing a detectable accumulation of protein on the sensor chip. The fastest αβTCR dissociation rate we have yet been able to directly measure by Biacore is 1.1 s^{-1} (half-life of 0.63 s) for the A6 αβTCR binding to HLA-A2/Tax with the peptide substitution Y8F (Baker et al., 2000). We can thus assume that the dissociation rate of the A6 αβTCR from P6A/HLA-A2 is at least as fast as 1.1 s^{-1} (corresponding to a half-life as short or shorter than 0.63 s), compared to a rate of 0.093 s^{-1} (half-life of 7.5 s) for dissociation from wild-type Tax/HLA-A2 (Table 1).

No Self-Association of αβTCR/Peptide/MHC Complexes Was Observed by Ultracentrifugation

We did not detect any TCR/peptide/MHC self-association into oligomeric complexes in the ultracentrifuge experiments, where self-association would be evident as a systematic deviation from the 1:1 binding model. This is in contrast to a report of self-association observed by light scattering for a complex between the mouse 2B4 αβTCR and the mouse class II MHC molecule I-E^k bound to a peptide from moth cytochrome c (MCC) (Reich et al., 1997). While our centrifuge experiments were performed at approximately the same temperature as the light scattering measurements (25°C versus 21°C), light scattering was performed at an ~10-fold higher concentration than the highest concentration used here for centrifugation (higher concentrations could not be used in the ultracentrifuge due to the limits of the optical system). However, the affinity of the A6 αβTCR for HLA-A2/Tax is 40-fold higher than the strongest reported affinity of the 2B4 αβTCR for I-E^k/MCC (Lyons et al., 1996; Reich et al., 1997). In solution, without any TCR or MHC oligomers present, self-association of TCR/peptide/MHC units would be linked to formation of the TCR/peptide/MHC complex. We can thus conclude that if self-association of the A6 αβTCR/Tax/HLA-A2 complex does occur, it is driven by an equilibrium weaker than that governing self-association of the 2B4 αβTCR/MCC/I-E^k complex. No self-association of free A6 αβTCR or HLA-A2/Tax was observed in control experiments with each protein alone (data not shown).

Alam et al. (1999) have provided evidence for TCR dimerization at 37°C using Biacore in the form of a greater response at 37°C than at 25°C; however, in their studies, it is unclear if the injected TCR concentration fully saturated the sensor chip at 25°C prior to the higher temperature injections. Initial analytical ultracentrifugation experiments at 37°C with the A6 αβTCR/Tax-peptide/HLA-A2 complex have not provided any evidence for dimerization at this temperature (B. B. and D. W., unpublished data).

Stepwise Repairing of a Packing Defect in the P6A Structure Restores αβTCR Binding Affinity

The interface between the αβTCR A6, Tax peptide, and HLA-A2 is populated by cavities and channels (Garboczi et al., 1996a; Ding et al., 1999). Upon substitution of proline 6 of the peptide with alanine, the cavity volume in the interface is increased by 38 $Å^3$. A water molecule is found in the enlarged cavity, hydrogen bonding to the alanine 6 amide nitrogen and occupying ~12 $Å^3$ (Ding et al., 1999) (Figures 2A and 2B). Accounting for the water, the actual increase in cavity volume with the P6A peptide is thus 26 $Å^3$. We attribute the loss in αβTCR affinity for the P6A ligand to this expanded cavity and bound water, as both internal cavities and bound water molecules are generally considered to be thermodynamically unfavorable (Eriksson et al., 1992; Dunitz et al., 1994).

As the increase in cavity volume with the P6A peptide results from removal of two methylenes of the proline side chain that had been cyclized to the position 6 nitrogen, we reasoned that αβTCR affinity should rise if the increase in cavity volume and fixing of the water molecule could be limited or prevented. We were also instructed by the mechanism of proline recognition by SH3 and WW domains, in which proline or an N-substituted amino acid is required for binding (Nguyen et al., 1998). We thus designed Tax variants in which position 6 was replaced with N-alkylated amino acids, varying the alkyl chain from one to three carbons (Figure 2E). Binding

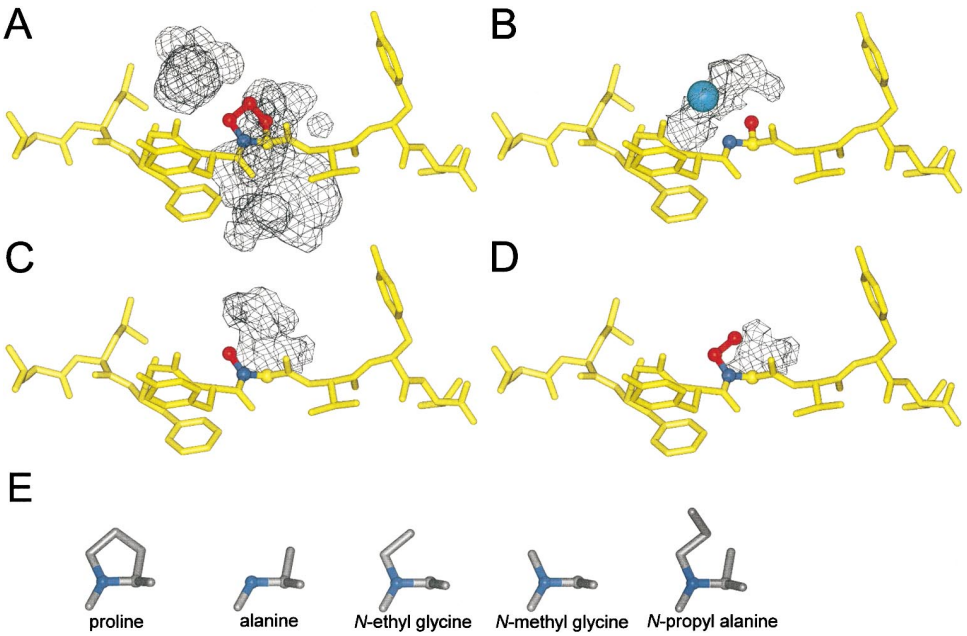

Figure 2. Cavity Space and Peptide Position 6 Substitutions

(A) Cavity space (mesh) around peptide position 6 in the structure with wild-type Tax. The orientation is such that the TCR is above the plane of the page and the MHC below. Proline 6 side chain is red; the amide nitrogen is blue.

(B) Increase in cavity volume (mesh) and bound water (cyan sphere) in the P6A structure relative to the structure with wild-type Tax. Orientation and coloring is the same as in (A).

(C and D) Increase in cavity volume (mesh) with P6MeG (C) and P6EtG (D) relative to the structure with wild-type Tax. Orientation and coloring is as in (A).

(E) Peptide position 6 substitutions used in this study. Amide nitrogen is blue.

of each modified-peptide/HLA-A2 complex to the A6 αβTCR was measured by Biacore and/or analytical ultracentrifugation. Figure 3 shows representative kinetic and equilibrium Biacore data; the results for each peptide are summarized in Table 1.

Tax-P6→N-Methyl Glycine

Tax with N-methyl glycine (sarcosine) at position 6 (P6MeG) has an αβTCR dissociation constant of 26 μM (centrifuge data) or a greater than 4-fold increase in affinity relative to P6A (Table 1). Unlike P6A, we could observe TCR binding with the P6MeG peptide using Biacore. The K_D from a Biacore equilibrium experiment, 27 μM, is identical within error to that obtained by analytical ultracentrifugation (Table 1). However, the αβTCR dissociation rate was still too fast to permit reliable kinetic measurements (Figure 3C).

Although the P6MeG peptide is missing the β carbon from position 6, it has a methyl group on the amide nitrogen that points directly toward the enlarged cavity (Figure 2C). It is likely that the bound water in the P6A structure is excluded from the cavity in the P6MeG peptide complex, as modeling indicates a steric clash between the N-methyl group and the bound water in the P6A complex.

Calculations with a modeled structure indicate that the increase in cavity volume with the P6MeG peptide relative to wild-type Tax is 39 Å^3, nearly identical to the increase in cavity volume with the P6A peptide (38 Å^3; because the β carbon of alanine was deleted and an N-methyl carbon added). The stronger αβTCR affinity for the P6MeG ligand relative to P6A is, thus, probably attributable to dissociation of the bound water, forced by methylation of the amide nitrogen.

Tax-P6→N-Ethyl Glycine

Tax with N-ethyl glycine at position 6 (P6EtG) has a TCR affinity of 2.1 μM (centrifuge data), or an ~60-fold increase over TCR affinity with the P6A peptide (116 μM) (Table 1). This peptide is similar to the P6MeG peptide, with an ethyl rather than a methyl group added to the amide nitrogen of position 6. Assuming the ethyl group is oriented similarly to the γ and δ carbons of the original proline side chain, this peptide completely fills the enlarged cavity created by the P6A substitution (Figure 2D). However, there is still a 13 Å^3 increase in cavity volume relative to the wild-type peptide, resulting from deletion of the β carbon, which is likely the main reason why TCR affinity with this peptide is slightly weaker than with wild-type.

Unlike P6A and P6MeG, high-quality kinetic data could be measured by Biacore with the P6EtG peptide (Figure 3A; values in Table 1). The αβTCR association rate (k_{on}) is 6.6 × 10^4 M^{-1} s^{-1}, ~1/2 of the rate observed with wild-type Tax. The dissociation rate (k_{off}) is 0.23 s^{-1}, corresponding to a TCR/peptide/MHC half-life of ~3 s. This is 2.5-fold shorter than the half-life of the complex with wild-type Tax (7.5 s; see Table 1). As discussed below, the half-life and TCR affinity of the P6EtG complex is almost but not quite equal to that of the Tax

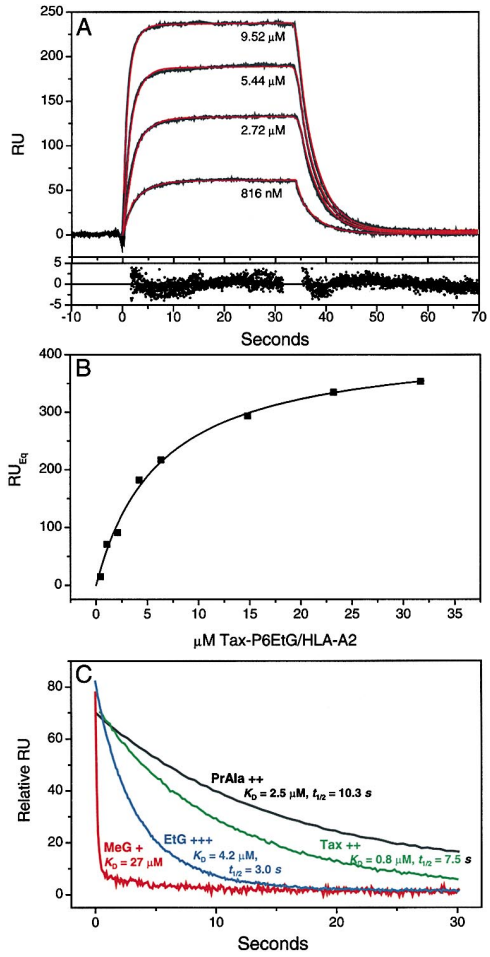

Figure 3. Representative Biacore Data

(A) Kinetic data for P6EtG/HLA-A2 binding to A6. Data are in black; red represents a fit to a 1:1 binding model. Concentrations of injected protein are indicated. Residuals for the fitted portions of the curve are beneath the data.

(B) Equilibrium binding data for P6EtG/HLA-A2 binding to A6. Line represents a fit to a 1:1 binding model (K_D = 4.2 μM).

(C) Representative dissociation phases from kinetic experiments. From left (fastest) to right (slowest): P6MeG, P6EtG, wild-type Tax, and P6PrA. The affinity of the MHC/peptide for the A6 TCR, the half-life of the TCR/peptide/MHC complex, and the relative cytotoxic potency of each ligand are indicated.

complex because the position 6 β carbon atom is missing.

Tax-P6→N-Propyl Alanine

As shown in Figures 2A and 2B, the packing defect observed with P6A results from the enlargement of the cavity adjacent to the position 6 side chain. Having demonstrated that "repairing" the packing defect with P6EtG can restore αβTCR binding affinity, we attempted to increase αβTCR affinity above that observed with wild-type Tax by filling cavity space found in the wild-type Tax complex near proline 6. By substituting N-propyl alanine at position 6 (P6PrA), we retained the β carbon as in alanine but added a third carbon to the N-alkyl substitution (Figure 2E). Modeling indicated that the propyl group could extend into the cavity near proline 6 present in the wild-type Tax complex if the β carbon of alanine were retained to prevent the propyl group from bending toward the α carbon to form a structure analogous to proline.

Although we aimed to reduce the cavity volume with the P6PrA peptide and, thus, increase αβTCR affinity, binding measurements indicated that the αβTCR affinity (K_D = 2.2 μM; Table 1) is slightly weaker than that observed for wild-type Tax (K_D = ~1 μM). Despite a weaker affinity, however, kinetic measurements show a longer half-life relative to wild-type Tax (P6PrA $t_{1/2}$ = 10.3 s, wild-type = 7.5 s). The longer half-life suggests that the P6PrA peptide achieves our goal of reducing the cavity space around position 6 but at the expense of an ~70% decrease in the association rate constant (from ~1.1 × 10^5 M^{-1} s^{-1} for Tax to ~0.3 × 10^5 M^{-1} s^{-1} for P6PrA), which results in a weaker TCR affinity. The decrease in k_{on} may be due to the need to fix the two torsion angles of the propyl group.

Thermodynamic Analysis of Cavity Volume and Bound Water

Binding of the A6 αβTCR to HLA-A2/Tax results in a conformational change in the peptide (Garboczi et al., 1996a). In the structure of HLA-A2/Tax without the αβTCR bound, the side chain of proline 6 is positioned away from the peptide binding groove (Madden et al., 1993); with the αβTCR bound, the proline is angled down into the groove. A water molecule found in the peptide binding groove beneath the proline must be displaced by this peptide conformational change (Khan et al., 2000). Presumably, displacing the bound water into the bulk solvent is thermodynamically favorable, contributing to the αβTCR binding affinity. When the A6 αβTCR binds the P6A ligand, the water is not forced out. Rather, it is retained in the peptide binding groove to hydrogen bond to the free amide nitrogen at P6, occupying ~12 Å^3 of the 38 Å^3 cavity created by the P6A substitution.

The $\Delta\Delta G^\circ$ between αβTCR binding to the P6A and P6MeG ligands is ~900 cal/mol ($\Delta\Delta G^\circ = -RT\ln K_{D1}/K_{D2}$). This includes contributions from an unfavorable net increase in cavity volume for P6MeG of 12 Å^3 (the volume of the water molecule displaced by the N-methylation) that at a free energy cost of cavity formation ranging from 24 to 33 cal/mol/Å^3 (Eriksson et al., 1992) would be only ~360 cal/mole. However, there are considerable uncertainties in estimating cavity effects (Eriksson et al., 1992). A favorable free energy gain is expected from release of the water, but its high B factor (50 Å^2) suggests that the entropic gain from its release is small (Dunitz et al., 1994). This analysis suggests that there may be a favorable enthalpy change associated with release of the water.

The $\Delta\Delta G^\circ$ between αβTCR binding to the P6MeG and P6EtG ligands, which differ by one methylene group, is ~1.5 kcal/mol. This agrees well with the value for the average stability loss incurred by deletion of methyl groups within the core of a protein (1.3 kcal/mol) (Jackson et al., 1993). The increase in cavity volume relative to the wild-type Tax peptide modeled with P6MeG is 39 Å^3; with P6EtG it is 13 Å^3, yielding a difference of 26 Å^3. If the only effect were due to the change in cavity

volume (this is unlikely as there may be small structural reorganizations with the N-substituted peptides), the free energy cost per cubic angstrom would be ~58 cal/mol, larger than the estimate of 24–33 cal/mol (Eriksson et al., 1992).

The $\Delta\Delta G^\circ$ from the K_D measurements of the αβTCR binding to the wild-type and P6EtG ligands is ~400 cal/mol. This is approximately what is expected from the increase of 13 Å^3 in cavity volume (~390 cal/mol). However, there could also be other effects, such as an entropic penalty from fixing the torsion angle in the ethyl group of P6EtG.

Finally, since TCR affinity can be restored to near wild-type level with a glycine-based N-alkylated amino acid at position 6, the loss of TCR binding affinity with the P6A peptide cannot be attributed to an entropic penalty resulting from increased flexibility of the peptide upon substituting proline with alanine; as to a first approximation, the backbone conformational entropy of an N-alkylated glycine should resemble that of alanine.

As Affinity Increases, TCR Antagonism Is Replaced by Weak and Then Full Agonism

The position 6 Tax variants were examined in a T cell assay measuring lysis of antigen-presenting cells (Figure 4A). As previously observed, P6A has little or no stimulatory activity, even when presented at concentrations several orders of magnitude above that required to elicit a response with wild-type Tax (Figure 4A, also Figure 2A in Ding et al., 1999). P6A is an antagonist if presented in 1000-fold excess over Tax (Figure 4B; also Figure 1F in Ding et al., 1999). The assays indicate that P6MeG is a weak agonist (not an antagonist; Figure 4B), while P6EtG and P6PrA are strong agonists (Figure 4A). The assay also indicates that P6EtG has a stimulatory activity even greater than wild-type Tax, an effect that was reproducible over several repeated experiments (Experimental Procedures). The same rank order, including the increased activity of P6EtG, was observed in cytokine release assays measuring IFN-γ and MIP-1β (data not shown).

Examination of TCR signaling by analysis of phosphorylation of the TCR-associated ζ chains and ZAP-70 (Figure 4C) demonstrates that Tax, P6EtG, and P6PrA stimulation induced a pattern of strong phosphorylation of the TCR-associated ζ chains and ZAP-70, a pattern typical of TCR signaling induced by agonists. T cell stimulation with P6MeG and P6A induced no detectable ZAP-70 phosphorylation and little ζ chain phosphorylation, a pattern typical of signaling by very weak agonists and antagonists (Sloan-Lancaster and Allen, 1996). We observed nearly identical patterns of ζ phosphorylation with the three agonist peptides, wild-type Tax, P6EtG, and P6PrA, despite the 3-fold range of TCR/peptide/MHC complex half-lives (10.3–3.0 s). This result contrasts with the ζ phosphorylation patterns seen with the mouse class II restricted αβTCR 3.L2, which were reported to vary considerably with MHC/peptide ligands with TCR affinities and half-lives of similar magnitude and range to those observed here (Kersh et al., 1998).

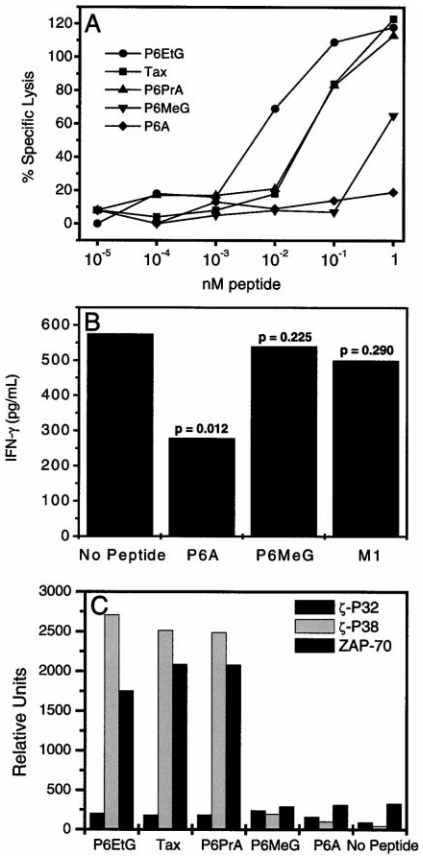

Figure 4. T Cell Assays

(A) Cytotoxicity of HLA-A2 targets pulsed with position 6 Tax peptide variants mediated by the A6 TCR-bearing clone 2G4. Effector: target ratio = 2.5:1. Identical rank ordering of activity was observed with IFN-γ and MIP-1β release as described in the text.

(B) P6A but not P6MeG antagonizes secretion of IFN-γ induced by the Tax peptide. The A6 TCR-bearing clone RS56 was cultured with antigen-presenting cells pulsed with 1000 nM candidate antagonist peptides (influenza M1 58–66 served as a negative control) for 2 hr at 37°C, and then, 1 nM Tax peptide was added. IFN-γ secretion was quantitated after 48 hr. Quantitative differences relative to the negative control were analyzed by the Student's t test.

(C) TCR signaling measured by phosphorylation of the TCR-associated ξ chains and ZAP-70. HLA-A2 antigen-presenting cells were pulsed with 10 μM of each peptide and used to stimulate the A6 TCR-bearing clone RS56. Results are presented as densitometry readings from an autoradiogram and are representative of two repeated experiments.

Discussion

Here, we studied variants of the HLA-A2/Tax agonist and HLA-A2/P6A antagonist ligands because the X-ray structures of the complexes of these two ligands with the A6 αβTCR are essentially identical (Ding et al., 1999), and there is no contact between either the position 6 proline or the alanine with the αβTCR (Garboczi et al., 1996a; Ding et al., 1999). Thus, alterations in the αβTCR structure were apparently not responsible for the very considerable difference in the TCR-initiated T cell signal. The only property of the interfaces that differed was an increase in cavity volume and a bound water molecule (not contacted by the αβTCR) in the P6A complex (Figures 2A and 2B). (The difference in solvation free energy between the proline- and alanine-containing peptide in the TCR-free HLA-Tax complex, calculated by molecular dynamics simulation, makes a significant contribution to the better binding of the wild-type to the TCR [O.

Michielin and M. Karplus, personal communication].) Using N-alkyl substitutions at position 6, we have in stepwise fashion filled in the part of the cavity occupied by the proline side chain, resulting in displacement of the bound water molecule. Consistent with our hypothesis that the enlarged cavity and bound water converted an agonist to an antagonist, the series of MHC/peptide ligands generated by N-alkyl substitution did, in stepwise fashion, restore agonist activity.

However, when the affinity of the series of MHC/peptide ligands for the αβTCR and the half-lives of the MHC/peptide/αβTCR complexes were measured, two anomalies were observed. Although the half-life of the P6PrA complex was longer than Tax (10.3 versus 7.5 s; Table 1; Figure 3C), they had the same potency (Figure 4A), and, although the half-life of the P6EtG was shorter than Tax (3 versus 7.5 s; Table 1; Figure 3C), it was a 10-fold more potent agonist (Figure 4A). These half-life differences are readily observed (Figure 3C) and accurately measurable (Table 1). In earlier studies of HLA-A2/peptide and H2-K^b/peptide ligands, half-life differences of 5- and 3-fold in the 1–10 s range are associated with 10,000- to 100,000-fold differences in agonist potency (as measured by the difference in peptide concentration required for half-maximal lysis or IL-2 production) (Udaka et al., 1996; Ding et al., 1999; Degano et al., 2000). Here, great care was taken to measure the kinetic constants accurately by fitting the data over the entire time range and correcting for bulk refractive index changes (Myszka, 1999). Furthermore, independent equilibrium and kinetic affinity measurements made with Biacore were consistent with each other and with affinity measurements made by sedimentation equilibrium analytical ultracentrifugation (Table 1).

Although many MHC/peptide ligands both from this study and others (Alam et al., 1996; Lyons et al., 1996; Kersh et al., 1998; Ding et al., 1999; Baker et al., 2000; Degano et al., 2000;) stimulate different T cell signals in proportion to the half-life of the complex they form with an αβTCR, a number of MHC/peptide combinations, including two studied here, do not fit this model. Examples include an antagonist ligand that formed αβTCR complexes with a half-life almost twice as long as that observed with a weak agonist ligand (Alam et al., 1996); three mutant-HLA-A2/Tax ligands that form αβTCR complexes with half-lives from 7 to 25 s, in the range of agonists, but which are weak agonists or null ligands (B. B., and D. W., unpublished data); an antagonist with 30-fold higher affinity than a weak agonist (Sykulev et al., 1998); an agonist with very weak TCR binding affinity (al-Ramadi et al., 1995); and the P6EtG/HLA-A2 and P6PrA/HLA-A2 ligands studied here, where the half-lives of the αβTCR complexes (Figure 3C; Table 1) do not correlate with the agonist potency (Figure 4A). Complicated binding kinetics have been observed for TCR binding to agonist ligands at 37°C (Alam et al., 1999) (the observations interpreted by Alam et al. [1999] as TCR dimerization would not have been observed here, as we did not perform experiments at 37°C, and the peptide/MHC was not attached to the Biacore chip). It remains to be determined if the anomalies observed here at 25°C remain at 37°C. It is a formal possibility that the P6EtG, P6PrA, and wild-type ligands will have different temperature dependencies and yield a better correlation of cytotoxic activity with half-life or affinity when measurements are performed at 37°C. However, the growing number of ligands whose potency does not correlate well with affinity and half-life suggests that other interpretations may have to be sought.

A limitation of X-ray structures and kinetic and thermodynamic measurements of MHC/peptide ligands with only the αβ chains of the TCR is that the CD3 and ζ subunits are lacking. Furthermore, the stoichiometry of the membrane-bound unliganded ground-state structure of the complete oligomeric TCR complex found on T cells is uncertain. Some evidence suggests that this complex contains two αβTCRs as well as CD3 and ζ subunits (Exley et al., 1995; San José et al., 1998; Fernández-Miguel et al., 1999; Cochran et al., 2000). The αβTCR/peptide/MHC interfaces observed crystallographically are probably good representations of those present with membrane-bound TCR because the study of many complexes has revealed good evidence of individualized induced fits between different αβTCRs and their ligands and between variant ligands and the same αβTCR (Garboczi et al., 1996a; Ding et al., 1998, 1999; Garcia et al., 1998; Reinherz et al., 1999; Degano et al., 2000; Hennecke et al., 2000). But, whether CD3, ζ, or the cell surface oligomeric state of the TCR place restraints on the disposition or conformation of the Cα and Cβ domains and/or the relationship of the V domains to the C domains is unknown.

Although the P6EtG and P6PrA complexes all have half-lives above a reasonable threshold for agonist activity, what is the physical basis for the relative differences in TCR signaling potency if there is no correlation with half-life or affinity? Apparently, there are two classes of MHC/peptide ligands based on the kinetic and thermodynamic data on ligand/αβTCR complexes: those ligands whose potency correlates with complex affinity and half-life and those ligands that do not. Models for the signaling mechanisms of those ligands whose potency correlates with half-life (or affinity) envision the peptide/MHC ligand stabilizing the TCR in a state that initiates signals by (for example) assembly to higher order structures or conformational changes (e.g., Janeway et al., 1989; McKeithan et al., 1995). All of the ligand/αβTCR X-ray structures have been interpreted to correlate, at least qualitatively, with the αβTCR affinities, but structural differences that would explain the anomalous cases of biological potency are not apparent. This raises the possibility that ligands whose potency does not correlate with the available measurements on isolated αβTCR would show different kinetic and thermodynamic effects on intact, oligomeric TCR. The biological potency of these ligands may be mediated by their effects on the structurally uncharacterized ground-state TCR. For example, if the ground-state cell surface TCR, before any ligand binds, contains two αβTCRs, the dimeric assembly may impose restraints on the individual αβTCRs that decrease their affinities for some ligands (like hemoglobin [Hb] does for oxygen) and increase their affinity for others (like Hb for Bohr protons) (Monod et al., 1965; Perutz, 1989).

Restraints imposed by oligomeric assemblies, such as those distinguishing tetrameric hemoglobin from a monomeric hemoglobin subunit, are the structural basis for cooperativity and allosteric regulation in proteins (Monod et al., 1965; Perutz, 1989). Such restraints can have profound effects on the affinities and kinetics of

ligand interactions; for example, monomeric hemoglobin subunits have a high affinity for oxygen, while the restraints of the tetrameric assembly (in the thermodynamically favored deoxy quarternary conformation) decrease the affinity of the same hemoglobin polypeptide chain by 25- to 500-fold (Dickerson and Geis, 1983). To date, all structural and detailed kinetic and thermodynamic measurements have been made on monomeric αβTCR. Oligomeric restraints on TCR might affect ligand kinetics or affinities. Some ligands may be able to bind the restrained state and induce it to change conformation to a less restrained conformation—a conformation, perhaps, similar to that seen in monomeric αβTCR. Such a mechanism has been described for molecular cooperativity in sequential models of allosteric control (Koshland et al., 1966). This proposal is similar to earlier suggestions that conformational changes play a role in TCR signaling (e.g., Janeway, 1995), the difference being that rather than a conformational change occurring in a receptor containing only one αβTCR, a change is proposed to occur as an unliganded oligomeric ground-state TCR complex transforms to a fully liganded complex. The existence of well-documented effects of ligands that do not fit models based on a monomeric αβTCR ground-state suggests that their explanation will require studies of the structure, thermodynamics, and kinetics of a putative oligomeric cooperative TCR entity.

Experimental Procedures

Proteins and Peptides

HLA-A2 and A6 αβTCR were refolded as soluble ectodomains from *E. coli* inclusion bodies as previously described (Garboczi et al., 1992, 1996b). Peptides were synthesized by Commonwealth Biotechnologies (Richmond, VA) and HPLC purified to > 95% purity. High peptide/MHC refolding yields indicated that peptide binding to the MHC was not impaired with any of the studied peptides.

The αβTCR used in all experiments contains the α and β chains up to and including the cysteines encoding the interchain disulfide bond, followed by a heterodimeric coiled coil (O'Shea et al., 1993) to stabilize the αβ dimer during refolding and analysis. A free cysteine is present at the C terminus of the β chain for coupling to a Biacore chip. Protein concentrations for all measurements were determined in triplicate and the average result used; extinction coefficients at 280 nm were 95,839 M^{-1} cm^{-1} for Tax/HLA-A2 and 84,503 M^{-1} cm^{-1} for the A6 TCR (Ding et al., 1999).

Analytical Ultracentrifugation

Analytical ultracentrifugation was performed using a Beckman XL-A instrument (Beckman, Palo Alto, CA). For analysis of individual proteins, three concentrations (MHC: 1, 3, and 7 μM; TCR: 1, 3, and 6 μM) of each protein were centrifuged at 12,500 and 15,000 rpm. Conditions were 10 mM phosphate, 150 mM NaCl (pH 7.4), and 25°C. Concentration versus position was recorded using absorbance at 280 nm. Equilibrium was assumed when subtraction of scans taken 4 hr apart showed no deviations. The six data sets for each sample were globally fit to the following equation using the program NONLIN (Johnson and Frasier, 1985):

$$A_r = A_0 \exp\left(M(1 - \bar{\nu}\rho)\frac{\omega^2}{RT}(x^2 - x_0^2)\right) + b \quad (1)$$

where A_r is the absorbance at radial position r; A_0 is the absorbance at the meniscus; M, the protein molecular weight; ω, the rotor angular velocity; RT, the product of the gas constant and temperature; x, the radial position; and b, a baseline offset. The variables A_0 and b were local parameters for each data set, whereas M was a global parameter. Partial specific volumes ($\bar{\nu}$) and solvent density (ρ) were calculated as described (Durchshlag, 1986). Fitted molecular weights were within 2% of the values calculated from sequence.

For measuring binding, three samples of proteins mixed at different concentrations were used. Concentrations were determined by preparing stocks of twice the desired value and mixing equal volumes; final concentrations were nearly equimolar and ranged from 3 to 9 μM. Samples were centrifuged as above, except that data were recorded at 255 nm. Data were analyzed with a 1:1 binding model:

$$c_r = dist\ A + dist\ B + c_{0A}c_{0B}\,\mathrm{K}\exp\left(M_{AB}(1 - \bar{\nu}_{AB}\rho)\frac{\omega^2}{RT}(x^2 - x_0^2)\right) + b \quad (2)$$

The terms *dist A* and *dist B* in Equation 2 represent the distribution of free TCR and peptide/MHC according to Equation 1 (excluding the baseline), except that data is expressed in terms of concentration, c. Absorbances were converted to concentrations during fitting using extinction coefficients at 255 nm. The third term in Equation 2 is the distrubution of the TCR/peptide/MHC complex; the reference concentration is the product of the free reference concentrations for the TCR and peptide/MHC and an equilibrium association constant, K ($K_D = 1/K$). The partial specific volume of the complex ($\bar{\nu}_{AB}$) was calculated as a weight average. Fitting was performed with reference concentrations and baselines as local parameters for each of the six data sets and with K as a global parameter. Due to overparameterization, it was necessary to exclude a reference concentration during fitting using the conservation of mass approach (Becerra et al., 1991). Cell boundaries were determined from scans at 360 nm where absorption was minimal. The fraction of TCR/peptide/MHC complexes present over the concentration ranges used ranged from ~1% to 4% for P6A/HLA-A2 to 28% to 64% for wild-type Tax/HLA-A2.

Surface Plasmon Resonance (Biacore)

Biacore measurements were performed using Biacore 1000 and 2000 instruments (Biacore, Uppsala, Sweden) as described (Ding et al., 1999). In brief, the TCR was coupled to a sensor chip using the free thiol engineered at the C terminus of the β chain. Equilibrium experiments were performed by injecting 70 μl of MHC/peptide at a flow of 10 μL/min. The response was determined by averaging the signal over the final 15 s of the injection and subtracting the response from an identical injection over a mock cysteine-coupled flowcell. Data were fit versus concentration to a 1:1 binding model. For kinetic experiments, 60 μl of MHC/peptide was injected at a flow of 100 μL/min. Identical injections over the mock flowcell were subtracted from the data. The entire association and dissociation phases were fit to a 1:1 binding model, excluding ~2 s at the beginning of each phase. As with our previous studies, we included a term for a small baseline drift during fitting (Ding et al., 1999; Baker et al., 2000). Inclusion of this term improved the residuals but had only a minor effect on the fitted parameters. Conditions for all experiments were 10 mM HEPES, 150 mM NaCl, 3 mM EDTA, 0.005% polysorbate-20 (pH 7.4), and 25°C. Injections were repeated twice. Fitting was performed using Biavaluation 3.0 (Biacore). For the equilibrium experiments, errors in Table 1 are the standard fitting error. Errors in kinetic constants are standard deviations from multiple determinations. Errors in half-lives and k_{on}/k_{off} values were determined by standard statistical error propagation.

Cavity Calculations

Cavity calculations were performed using the program SURFNET (Laskowski, 1995). All atoms of the TCR Vα/Vβ and MHC α1/α2 domains and the peptide were included in the calculations; volume changes were calculated as differences in total cavity volume. Structures were modeled by adding or removing atoms from the structure of the complex with the wild-type Tax peptide (Protein Data Bank entry 1AO7). Similar results were obtained using the structure with the P6A peptide (Protein Data Bank entry 1QRN) as the starting structure. Optimum, minimum, and maximum probe radii were found by varying the parameters until further changes produced no significant changes in difference cavity volumes. Grid spacing was 0.6 Å. The increase in cavity volume with P6A is larger than previously reported (Ding et al., 1999); our previous report underestimated the increase in cavity volume as the calculations were restricted to only

the atoms of peptide position 6 and the MHC $\alpha1/\alpha2$ domains. As SURFNET uses atom pairs to calculate cavities, limiting the calculation in this manner results in an incomplete exploration of cavity space.

Figures 2B through 2D represent actual changes in cavity volume and were generated with the MAPDIFF program distributed with SURFNET using results from the calculations of total cavity volume. To make Figure 2A, the calculation was limited to the atoms of proline 6 (excluding the carbonyl) and all atoms of the TCR $V\alpha/V\beta$ and MHC $\alpha1/\alpha2$ domains. This simplification allows visualization of only the regions of cavity space in the A6 TCR/Tax/HLA-A2 interface that are adjacent to proline 6.

T Cell Assays

Cytotoxicity was quantitated with a fluorometric assay using HLA-A2-transfected cells as previously described (Ding et al., 1998). Effector cells were the A6-expressing $CD8^+$ T cell clone 2G4 (Utz et al., 1996). IFN-γ, MIP-1β, and antagonism assays were performed using the A6-expressing $CD8^+$ T cell clone RS56 as previously described (Utz et al., 1996; Ding et al., 1999). TCR-associated signaling was assayed with anti-phospho-tyrosine antibodies and quantitated with densitometry as described (Ding et al., 1999).

P6EtG had higher activity than wild-type Tax in the cytotoxicity, IFN-γ, and MIP-1β assays. The assays were repeated several times with different peptide stocks, and each time the same result was observed. This cannot be attributed to small errors in peptide concentration, as the assays are performed on a logarithmic scale. All peptides were prepared in the same fashion, purified by HPLC, and appeared to have comparable solubilities. An attempt to limit potential peptide proteolysis by performing the experiments in serum-free conditions produced the same hierarchy of peptide activity, indicating differential proteolysis from proteases that may be present in serum is not a contributing factor.

Acknowledgments

We thank A. Haykov, C. Garnett, and R. Turner for technical support and O. Michielin and M. Karplus for sharing unpublished data. This work was supported by the National Institutes of Health and the Howard Hughes Medical Institute (HHMI). B. M. B. is supported by a postdoctoral fellowship from the Cancer Research Institute. D. C. W. is an investigator of the HHMI.

Received May 17, 2000; revised September 6, 2000.

References

Alam, S.M., Travers, P.J., Wung, J.L., Nasholds, W., Redpath, S., Jameson, S.C., and Gascoigne, N.R.J. (1996). T-cell receptor affinity and thymocyte positive selection. Nature *381*, 616–620.

Alam, S.M., Davies, G.M., Lin, C.M., Zal, T., Nasholds, W., Jameson, S.C., Hogquist, K.A., Gascoigne, N.R.J., and Travers, P.J. (1999). Qualitative and quantitative differences in T cell receptor binding of agonist and antagonist ligands. Immunity *10*, 227–237.

al-Ramadi, B.K., Jelnoek, M.T., Boyd, L.F., Margulies, D.H., and Bothwell, A.L. (1995). Lack of strict correlation of functional sensitization with the apparent affinity of MHC/peptide complexes for the TCR. J. Immunol. *155*, 662–673.

Baker, B.M., Ding, Y.H., Garboczi, D.N., Biddison, W.E., and Wiley, D.C. (2000). Structural, biochemical, and biophysical studies of HLA-A2/altered peptide ligands binding to viral-peptide-specific human T-cell receptors. Cold Spring Harb. Symp. Quant. Biol. *64*, 235–241.

Becerra, S.P., Kumar, A., Lewis, M.S., Widen, S.G., Abbots, J., Karawya, E.M., Hughes, S.H., Shiloach, J., and Wilson, S.H. (1991). Protein-protein interactions of HIV-1 reverse transcriptase: implication of central and C-terminal regions in subunit binding. Biochemistry *30*, 11707–11719.

Cochran, J.R., Cameron, T.O., and Stern, L.J. (2000). The relationship of MHC-peptide binding and T cell activation probed using chemically defined MHC class II oligomers. Immunity *12*, 241–250.

Degano, M., Garcia, K.C., Apostolopoulos, V., Rudolph, M.G., Teyton, L., and Wilson, I.A. (2000). A functional hot spot for antigen recognition in a superagonist TCR/MHC complex. Immunity *12*, 251–261.

Dickerson, R.E., and Geis, I. (1983). Hemoglobin: Structure, Function, Evolution and Pathology. (Menlo Park, CA: Benjamin/Cummings, Inc.).

Ding, Y.H., Smith, K.J., Garboczi, D.N., Utz, U., Biddison, W.E., and Wiley, D.C. (1998). Two human T cell receptors bind in a similar diagonal mode to the HLA-A2/Tax peptide complex using different TCR amino acids. Immunity *8*, 403–411.

Ding, Y.H., Baker, B.M., Garboczi, D.N., Biddison, W.E., and Wiley, D.C. (1999). Four A6-TCR/peptide/HLA-A2 structures that generate very different T cell signals are nearly identical. Immunity *11*, 45–56.

Dunitz, J.D. (1994). The entropic cost of bound water in crystals and biomolecules. Science *264*, 670–670.

Durchshlag, H. (1986). Thermodynamic Data for Biochemistry and Biotechnology. (New York: Springer-Verlag).

Eriksson, A.E., Baase, W.A., Zhang, X.J., Heinz, D.W., Blaber, M., Baldwin, E.P., and Matthews, B.W. (1992). Response to a protein structure to cavity-creating mutations and its relation to the hydrophobic effect. Science *255*, 178–183.

Exley, M., Wileman, T., Mueller, B., and Terhorst, C. (1995). Evidence for multivalent structure of T-cell antigen receptor complex. Mol. Immunol. *32*, 829–839.

Fernández-Miguel, G., Alarcón, B., Iglesias, A., Bluethmann, H., Alvarez-Mon, M., Sanz, E., and de la Hera, A. (1999). Multivalent structure of an $\alpha\beta$T cell receptor. Proc. Natl. Acad. Sci. USA *96*, 1547–1552.

Garboczi, D.N., Hung, D.T., and Wiley, D.C. (1992). HLA-A2-peptide complexes: refolding and crystallization of molecules expressed in *Escherichia coli* and complexed with single antigenic peptides. Proc. Natl. Acad. Sci. USA *89*, 3429–3433.

Garboczi, D.N., Ghosh, P., Utz, U., Fan, Q.R., Biddison, W.E., and Wiley, D.C. (1996a). Structure of the complex between T-cell receptor, viral peptide, and HLA-A2. Nature *384*, 134–141.

Garboczi, D.N., Utz, U., Ghosh, P., Seth, A., Kim, J., van Tienhoven, A.E., Biddison, W.E., and Wiley, D.C. (1996b). Assembly, specific binding, and crystallization of a human TCR-$\alpha\beta$ with an antigenic tax peptide from human T lymphotropic virus type 1 and the class I MHC molecule HLA-A2. J. Immunol. *157*, 5403–5410.

Garcia, K.C., Degano, M., Pease, L.R., Huang, M., Peterson, P.A., Teyton, L., and Wilson, I.A. (1998). Structural basis of plasticity in T cell receptor recognition of a self peptide-MHC antigen. Science *279*, 1166–1172.

Hausmann, S., Biddison, W.E., Smith, K.J., Ding, Y.H., Garboczi, D.N., Utz, U., Wiley, D.C., and Wucherpfennig, K.W. (1999). Peptide recognition by two HLA-A2/Tax11-19-specific T cell clones in relationship to their MHC/peptide/TCR crystal structures. J. Immunol. *162*, 5389–5397.

Hennecke, J., Carfi, A., and Wiley, D.C. (2000). Structure of a covalently stabilized complex of a human $\alpha\beta$ T cell receptor, influenza HA peptide, and MHC class II molecule, HLA-DR1. EMBO J., in press.

Jackson, S.E., Moracci, M., elMasry, N., Johnson, C.M., and Fersht, A.R. (1993). Effect of cavity-creating mutations in the hydrophobic core of chymotrypsin inhibitor 2. Biochemistry *32*, 11259–11269.

Janeway, C.A., Jr. (1995). Ligands for the T-cell receptor: hard times for avidity models. Immunol. Today *16*, 223–225.

Janeway, C.A., Jr., Dianzani, U., Portoles, P., Rath, S., Reich, E.P., Rojo, J., Vagi, J., and Murphy, D.P. (1989). Cross-linking and conformational change in T-cell receptors: role in activation and in repertoire selection. Cold Spring Harbor Symp. Quant. Biol. *54*, 657–666.

Johnson, M.L., and Frasier, S.G. (1985). Nonlinear least-squares analysis. Methods Enzymol. *117*, 301–342.

Kersh, G.J., Kersh, E.N., Fremont, D.H., and Allen, P.M. (1998). High- and low-potency ligands with similar affinities for the TCR: the importance of kinetics in TCR signaling. Immunity *9*, 817–826.

Khan, A.R., Baker, B.M., Ghosh, P., Biddison, W.E., and Wiley, D.C. (2000). The structure and stability of an HLA-A201/Octameric Tax

peptide complex with an empty conserved peptide-N-terminal binding site. J. Immunol. *164*, 6398–6405.

Koshland, D.E., Jr., Neméthy, G., and Filmer, D. (1966). Comparison of experimental binding data and theoretical models in proteins containing subunits. Biochemistry *10*, 365–385.

Laskowski, R.A. (1995). SURFNET: a program for visualizing molecular surfaces, cavities, and intermolecular interactions. J. Mol. Graph. *13*, 323–330.

Lyons, D.S., Lieberman, S.A., Hampl, J., Boniface, J.J., Chien, Y., Berg, L.J., and Davis, M.M. (1996). A TCR binds to antagonist ligands with lower affinities and faster dissociation rates than to agonists. Immunity *5*, 53–61.

Madden, D.R., Garboczi, D.N., and Wiley, D.C. (1993). The antigenic identity of peptide-MHC complexes: a comparison of the conformations of five viral peptides presented by HLA-A2. Cell *75*, 693–708.

Matsui, K., Boniface, J.J., Steffner, P., Reay, P.A., and Davis, M.M. (1994). Kinetics of the T-cell receptor binding to peptide/I-K^k complexes: correlation of the dissociation rate with T-cell responsiveness. Proc. Natl. Acad. Sci. USA *91*, 12862–12866.

McKeithan, T.W. (1995). Kinetic proofreading in T-cell receptor signal transduction. Proc. Natl. Acad. Sci. USA *92*, 5042–5046.

Monod, J., Wyman, J., and Changeux, J.P. (1965). On the nature of allosteric transitions: a plausible model. J. Mol. Biol. *12*, 88–118.

Myszka, D.G. (1999). Improving biosensor analysis. J. Mol. Recognit. *12*, 279–284.

Nguyen, J.T., Turck, C.W., Cohen, F.E., Zuckermann, R., and Lim, W.A. (1998). Exploiting the basis of proline recognition by SH3 and WW domains: design of N-substituted inhibitors. Science *282*, 2088–2091.

O'Shea, E.K., Lumb, K.J., and Kim, P.S. (1993). Peptide velcro: design of a heterodimeric coiled coil. Curr. Biol. *3*, 658–667.

Perutz, M.F. (1989). Mechanisms of cooperativity and allosteric regulation in proteins. Q. Rev. Biophys. *22*, 139–236.

Reich, Z., Boniface, J.J., Lyons, D.S., Borochov, N., Wachtel, E.J., and Davis, M.M. (1997). Ligand-specific oligomerization of T-cell receptor molecules. Nature *387*, 617–620.

Reinherz, E., Tan, K., Tang, L., Kern, P., Liu, J., Xion, Y., Hussey, R.E., Smolyar, A., Hare, B., Zhang, R., et al. (1999). The crystal structure of a T cell receptor in complex with peptide and MHC class II. Science *286*, 1913–1921.

San José, E., Sahuquillo, A.G., Bragado, R., and Alarcón, B. (1998). Assembly of the TCR/CD3 complex: CD3ϵ/δ and CD3ϵ/γ dimers associate indistinctly with both TCRα and TCRβ chains. Evidence for a double TCR heterodimer model. Eur. J. Immunol. *28*, 12–21.

Sloan-Lancaster, J., and Allen, P.M. (1996). Altered peptide ligand-induced partial T cell activation: molecular mechanisms and role in T cell biology. Annu. Rev. Immunol *14*, 1–27.

Sykulev, Y., Vugmeyster, Y., Brunmark, A., Ploegh, H.L., and Eisen, H.N. (1998). Peptide antagonism and T cell receptor interactions with peptide-MHC complexes. Immunity *9*, 475–483.

Udaka, K., Wiesmüller, K., Kienle, S., Jung, G., and Walden, P. (1996). Self-MHC-restricted recognized by an alloreactive T lymphocyte clone. J. Immunol. *157*, 670–678.

Utz, U., Banks, D., Jacobson, S., and Biddison, W.E. (1996). Analysis of the T-cell repertoire of human T-cell leukemia virus type 1 (HTLV-1) Tax peptide-specific $CD8^+$ cytotoxic T lymphocytes from patients with HTLV-1 associated disease: evidence for oligoclonal expansion. J. Virol. *70*, 843–851.

van der Merwe, P.A., Barclay, A.N., Mason, D.W., Davies, E.A., Morgan, B.P., Tone, M., Krishnam, A.K., Ianelli, C., and Davis, S.J. (1994). Human cell-adhesion molecule CD2 binds CD58 (LFA-3) with a very low affinity and an extremely fast dissociation rate but does not bind CD48 or CD59. Biochemistry *33*, 10149–10160.